

Theoretical treatment of the nonlinear anelastic internal friction peaks appearing in the cold-worked Al-based solid solutions

Q. F. Fang

Laboratory of Internal Friction and Defects in Solids, Institute of Solid State Physics, Chinese Academy of Sciences, 230031 Hefei, China

(Received 21 October 1996; revised manuscript received 21 January 1997)

The longitudinal and transverse diffusion equations of solute atoms along the dislocation core formulated based on the dislocation kink model are solved with the numerical difference method. The theoretical internal friction and modulus defect curves versus temperature and strain amplitude were calculated for the nonlinear anelastic internal friction peaks (P_0 , P_1' , and P_1'' peaks). The manifestations of these curves are compared with the experimental results previously obtained in cold-worked Al-Mg and Al-Cu solid solutions around room temperature. [S0163-1829(97)04025-3]

I. INTRODUCTION

The nonlinear effect or strain amplitude dependence of the internal friction (IF) is a universal phenomenon at a relatively high strain level, which is mainly due to the nonlinear interaction between defects in materials. At a very low strain amplitude, the IF is amplitude independent as pointed out by the linear anelasticity. In a higher-strain-amplitude range, however, the IF is generally amplitude dependent. In general, there are two types of amplitude-dependent IF. One increases monotonously with an increase of the strain amplitude and can be explained quite well by the model of dislocation breakaway [Granato-Lücke (GL) model] in which the point defects interacting with the dislocation are treated as immobile pinners.¹ The other, which was observed by $K\hat{e}^2$ in cold-worked Al-Cu solid solutions and attributed to a model of dislocation dragging the mobile point defects (solute atoms), increases at first with the increase of the strain amplitude and decreases after passing a maximum, exhibiting an amplitude peak when the IF is plotted as a function of strain amplitude. Because it exhibits at the same time a temperature peak of the relaxation type, it is thus assigned by $K\hat{e}^3$ with the name of "nonlinear anelastic IF peak" and the characteristics related to this phenomenon are called "nonlinear anelasticity."

In a previous paper by $K\hat{e}^4$, the mathematical analysis of the dislocation core diffusion of point defects by Winkler-Gniewek *et al.*⁵ (designated as the WG model) on the basis of a double-loop string model was described. It was shown that the theoretical IF curves derived by WG conform, in a certain extent, to the manifestations of the nonlinear anelastic IF peaks appearing in cold-worked Al-Cu and Al-Mg specimens around room temperature which were attributed to the dislocation core diffusion. However, it was pointed out that the physical picture on the basis of the string model is not clear, especially for the transverse core diffusion.

Recently, the diffusion equations of the solute atom along the dislocation core were figured out on the basis of the dislocation kink model.^{6,7} The relaxation time and the relaxation strength associated with the longitudinal and transverse core diffusion of solute atoms under quasistatic stress have

been computed by analytically solving the diffusion equation and were found to be nonlinear with respect to the applied stress amplitude. However, the IF and modulus defect obtained by assuming the relaxation process to be nearly a Debye type with nonlinear relaxation time and relaxation strength are approximate in the case of the amplitude-dependent IF.⁷ To check the model more quantitatively, a more accurate method must be applied; i.e., these equations must be solved under the case of sinusoidal external stress.

In this paper the diffusion equations of the solute atom along the dislocation core for the three peaks are solved with the numerical difference method in the case of externally applied sinusoidal stress. The manifestation of the derived theoretical curves of the IF and modulus defect is quite different from that obtained by the approximate method in Ref. 7, but to a greater extent consistent with experimental results previously obtained.

II. THEORETICAL TREATMENTS

A. Diffusion equation of the solute atom along dislocation core

In the case of the P_1' peak, the diffusion equation and its initial and boundary condition can be rewritten in the following form when a quasistatic external stress is applied:⁶ Diffusion equation:

$$\frac{\partial \rho_L}{\partial t} = \frac{D_{L1}}{L^2} \frac{\partial}{\partial \xi} \left(\frac{\partial \rho_L}{\partial \xi} - \alpha^2 \xi \rho_L \right); \quad (1)$$

boundary condition:

$$\left[\frac{\partial \rho_L}{\partial \xi} - \alpha^2 \rho_L \right]_{\xi=+1} = \left[\frac{\partial \rho_L}{\partial \xi} + \alpha^2 \rho_L \right]_{\xi=-1} = 0; \quad (2)$$

normalized condition:

$$\int_{-1}^{+1} L \rho_L(\xi, t) d\xi = 1; \quad (3)$$

initial condition:

$$\rho_L(\xi, 0) = \frac{1}{2L}, \quad (4)$$

where

$$\alpha^2 = \frac{3(\sigma bh)^2 L^3}{4PkT}, \quad \xi = \frac{x}{L}, \quad (5)$$

and k is Boltzmann constant, T is the absolute temperature, t is the time, b is the magnitude of the Burger's vector, h is the height of kinks, L is the dislocation segment length, coordinates x and y are along and perpendicular to the dislocation line, respectively, D_{L1} is the longitudinal core diffusion coefficient of the solute atom situated on the middle of the kink, and $\rho_L(\xi, t)$ is the longitudinal distribution function of the solute atoms in the dislocation core and relates to the total distribution function $\rho(\xi, y, t)$ by

$$\rho(\xi, y, t) = \rho_L(\xi, t) \sqrt{\frac{\beta}{2\pi kT}} \exp\left[-\frac{\beta(y-y_0)^2}{2kT}\right]. \quad (6)$$

The anelastic strain can be calculated by

$$\varepsilon_A(t) = \frac{3\Lambda\sigma(bh)^2 L^2}{4P} \left[\frac{7}{9} + L \int_{-1}^{+1} \rho_L(\xi, t) \xi^2 d\xi \right]. \quad (7)$$

In the case of a sinusoidal external stress, the results stated above are still true, as long as the changing frequency of the external stress is very low, e.g., in the low-frequency IF measurement. Therefore, we can simply substitute σ with $\sigma = \sigma_0 \sin\omega t$ in Eqs. (1)–(7) in the case of sinusoidal external stress.

In the case of P_0 and P_1' peaks, the diffusion equation and the initial and boundary conditions can be rewritten as follows (only in the case of sinusoidal external stress $\sigma = \sigma_0 \sin\omega t$): diffusion equation:

$$\frac{\partial \rho_L}{\partial t} = \frac{D_{L2}}{L^2} \frac{\partial}{\partial \xi} \left(\frac{\partial \rho_L}{\partial \xi} - f \rho_L \right); \quad (8)$$

boundary condition:

$$\left[\frac{\partial \rho_L}{\partial \xi} - f \rho_L \right]_{\xi=+1} = \left[\frac{\partial \rho_L}{\partial \xi} + f \rho_L \right]_{\xi=-1} = 0; \quad (9)$$

normalized condition:

$$\int_{-1}^{+1} L \rho_L(\xi, t) d\xi = 1; \quad (10)$$

initial condition:

$$\rho_L(\xi, 0) = \frac{1}{2L}, \quad (11)$$

where

$$f = 2\alpha_0^2 \xi \sin^2 \omega t - \frac{\alpha_0^2}{2} \xi \cos^2 \phi \sin^2(\omega t - \phi) + \gamma_0 \sin(\phi) \cos(\omega t - \phi), \quad (12)$$

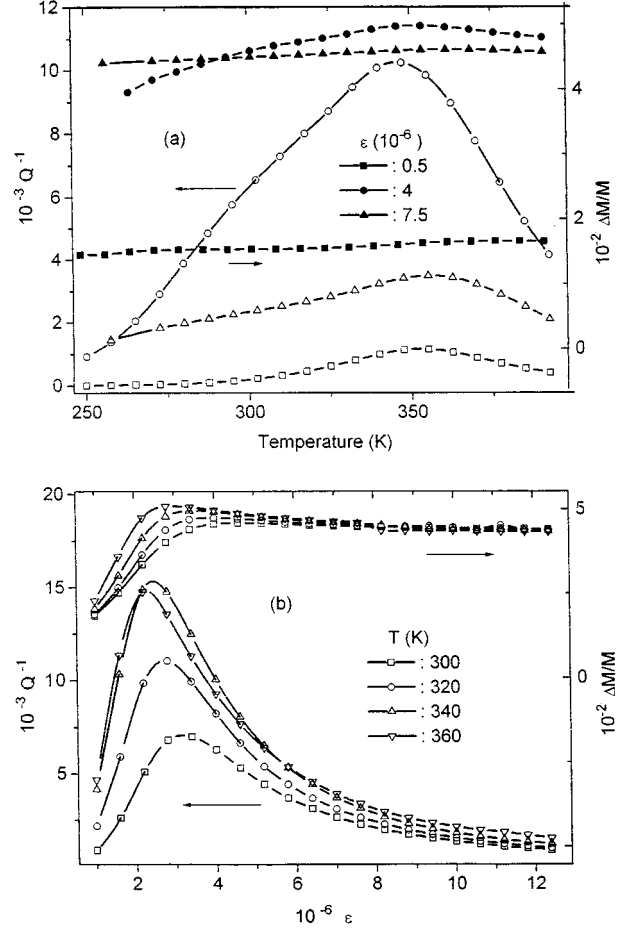


FIG. 1. Internal friction and modulus defect curves of the P_1' peak vs temperature (a) and strain amplitude (b). In (a), curves 1–3 correspond to the strain amplitude $0.5, 4,$ and 7.5×10^{-6} , respectively; in (b), curves 1–4 correspond to the temperature $300, 320, 340,$ and 360 K, respectively.

$$\alpha_0^2 = \frac{(\sigma_0 bh)^2 L^3}{PkT}, \quad \gamma_0 = \frac{\sigma_0 b L^2}{kT} \tan \theta,$$

$$\tan \phi = \omega \tau_T = \frac{\omega h^2 kT}{2PLD_T} (L^2 - x^2),$$

and D_{L2} and D_T are the longitudinal and transverse core diffusion coefficients of the solute atom situated on the extremities of the kink, respectively.

The total distribution function $\rho(\xi, y, t)$ is now the form

$$\rho(\xi, y, t) = \rho_L(\xi, t) \sqrt{\frac{\beta}{2\pi kT}} \exp\left[-\frac{\beta[y - \delta(t)]^2}{2kT}\right], \quad (13)$$

where

$$\delta(t) = \cos \phi \frac{\sigma_0 b L}{\beta kT} \sin(\omega t - \phi). \quad (14)$$

The anelastic strain can be calculated by the equation

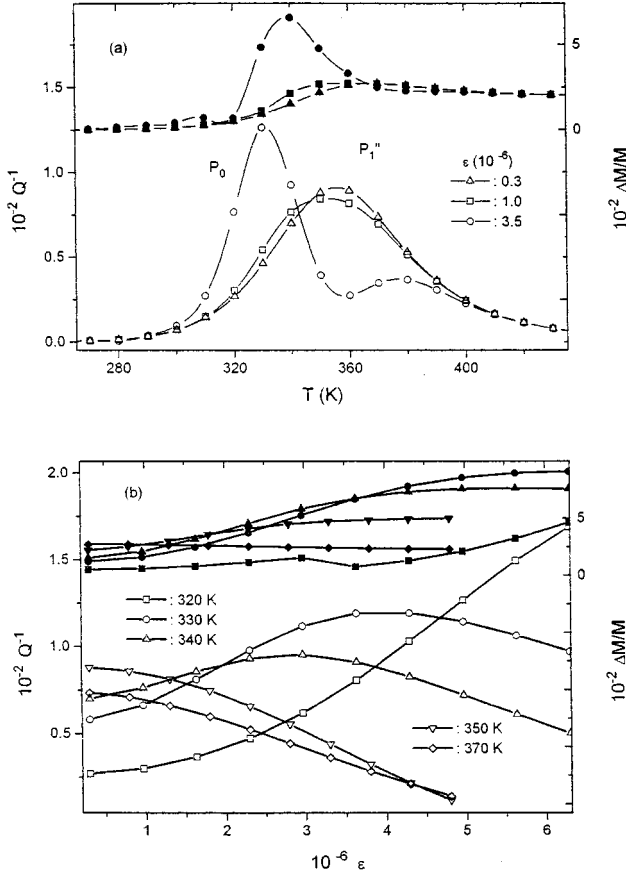


FIG. 2. Internal friction and modulus defect curves of the P_0 and P_1'' peaks vs temperature (a) and strain amplitude (b). In (a), curves 1–3 correspond to the strain amplitude 0.3, 1, and 3.5×10^{-6} , respectively; in (b), curves 1–5 correspond to the temperature 320, 330, 340, 350, and 370 K, respectively.

$$\begin{aligned} \varepsilon_A(t) &= \frac{\Lambda b}{2} \int_{-1}^1 d\xi \int_{-\infty}^{\infty} dy S \rho_L(\xi, t) \rho_T(\xi, y, t) \\ &= \Lambda L^3 \frac{\sigma_0 (bh)^2}{4P} \int_{-1}^1 [4\xi^2 \sin \omega t + (1 - \xi^2) \cos \phi \\ &\quad \times \sin(\omega t - \phi)] \rho_L(\xi, t) d\xi + \frac{\Lambda \sigma_0 (bhL)^2}{3P} \sin \omega t. \end{aligned} \quad (15)$$

B. Internal friction and modulus defect of the P_0 , P_1' , and P_1'' peaks

To calculate the IF and modulus defect under a periodical external stress, $\sigma = \sigma_0 \sin \omega t$, the partial differential equation (1) or (8) with its initial and boundary conditions (2)–(5) or (9)–(12) must be solved numerically, and then the strain produced by the sidewise motion of the kink chain as a function of time can be obtained from Eq. (7) or (15). A definite difference method is adopted to integrate the longitudinal distribution function with small steps of time and x coordinate, and the IF and modulus defect can thus be computed by the following equations.

The dissipated elastic energy per vibration cycle is

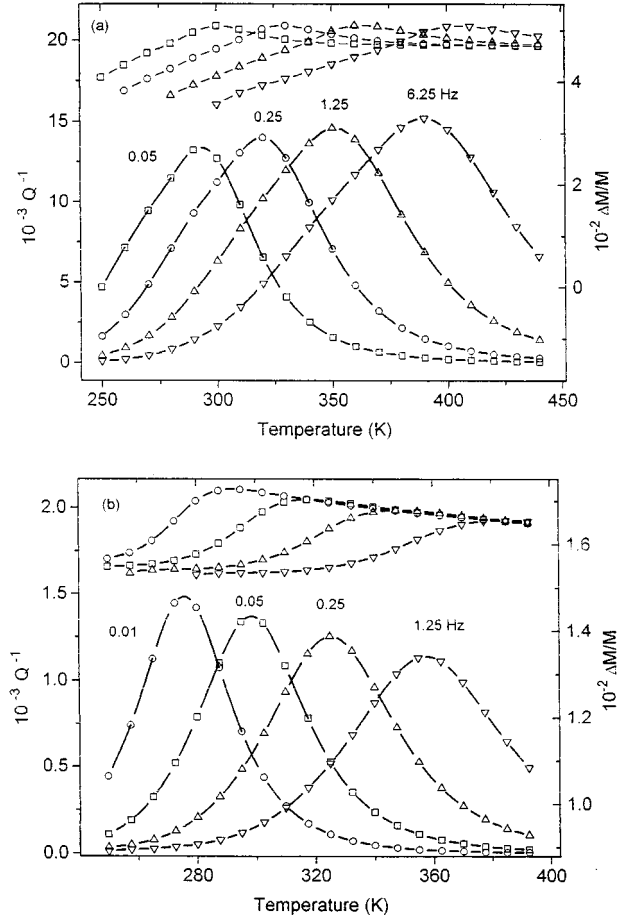


FIG. 3. Internal friction and modulus defect curves of the P_1' peak vs temperature at various frequencies for two strain amplitudes of 3×10^{-6} (a) and 0.5×10^{-6} (b). Curves 1–4 in (a) correspond to different frequencies 0.05, 0.25, 1.25, and 6.25 Hz, respectively, and curves 1–4 in (b) correspond to different frequencies 0.01, 0.05, 0.25, and 1.25 Hz, respectively.

$$\begin{aligned} \Delta W &= \oint \sigma d\varepsilon = - \oint \varepsilon d\sigma \\ &= -\sigma_0 \sum_{j=0}^{2\pi/\Delta t} \cos(j\Delta t) \varepsilon(j\Delta t) \Delta t. \end{aligned} \quad (16)$$

The stored elastic energy equals to the work done by the applied stress in the first quarter of a vibration cycle minus a quarter of the dissipated elastic energy:

$$\begin{aligned} W &= \int_0^{\pi/2} \sigma d\varepsilon - \frac{\Delta W}{4} \\ &= \sigma_0 \varepsilon \left(\frac{\pi}{2\Delta t} \right) - \sigma_0 \sum_{j=0}^{\pi/2\Delta t} \cos(j\Delta t) \varepsilon(j\Delta t) \Delta t - \frac{\Delta W}{4}. \end{aligned} \quad (17)$$

Internal friction is by definition

$$Q^{-1} = \frac{\Delta W}{2\pi W}. \quad (18)$$

Modulus defect is by definition

$$\frac{\Delta M}{M} = \frac{2GW}{\sigma_0^2} - 1, \quad (19)$$

where Δt is the integration step of the time variable $t' = \omega t$ used in the process of solving the partial differential equation and $\varepsilon(t') = \varepsilon_A(t') + \sigma/G$ is the total strain.

III. RESULTS

By numerical calculation, we take the typical parameters in Al crystal: $\Lambda L^2 = 0.01$, $Gb^3 = 5$ eV, and $L = 10^3$ b. The measurement frequency f is set to be 1 Hz. Concerning D_L and D_T , we have

$$D_{L1} = D_{L10} \exp\left(-\frac{H_{L1}}{kT}\right), \quad D_{L2} = D_{L20} \exp\left(-\frac{H_{L2}}{kT}\right),$$

$$D_T = D_{\tau 0} \exp\left(-\frac{H_\tau}{kT}\right),$$

and take $H_{L1} = H_{L2} = 0.5$ eV and $H_\tau = 0.6$ eV.⁸ The values of D_{L10} , D_{L20} , and $D_{\tau 0}$ were chosen so that the optimum temperature of P_0 , and P'_1 , and P''_1 peak is, respectively, 320, 340, and 360 K at $\sigma_0 \approx 0$ (extrapolated) and $f = 1$ Hz.

In Fig. 1 are given the variations of the IF and modulus defect versus temperature (a) and strain amplitude (b) for the P'_1 peak. As the strain amplitude increases, the P'_1 peak increases at first and then decreases in height and hardly changes position, as shown in Fig. 1(a). This feature of the P'_1 peak is contrary to that predicted by the approximate method in Ref. 7, but does appear in our recent experiment. At a very low strain amplitude, the P'_1 peak is nearly a standard Debye peak as considered approximately in Ref. 7, but at high strain amplitude, the P'_1 peak is very broad and becomes asymmetrical, as can be seen apparently in Fig. 1(a), which is in accordance with the experimental results in Ref. 9. The modulus defect increases with the increase of temperature (a) or strain amplitude (b). The strain amplitude IF curve shown in Fig. 1(b) reaches a very low value at the higher-strain-amplitude side and its peak position shifts toward a lower strain amplitude as the temperature increases. Although the shift direction of the amplitude peak with tem-

perature is same as that of Ref. 7, its shift amount is much smaller and is more consistent with the experimental results of the P'_1 peak in Al-Mg solid solutions.⁹

Figure 2 shows the variations of the IF and modulus defect versus temperature (a) and strain amplitude (b) for P_0 and P''_1 peaks. At a low strain amplitude, the two peaks (P_0 and P''_1) overlap each other. The P_0 peak is very small, while the P''_1 peak is relatively large. The modulus defect for the two peaks increases with the increase of temperature. As the strain amplitude increases, the P_0 peak shifts toward lower temperature and increases in height. In contrast, the P''_1 peak shifts toward higher temperature and decreases. At a relatively high strain amplitude, the modulus defect increases at first and then decreases with the increase of temperature, showing an abnormal effect. In the temperature range of the P_0 peak, the amplitude IF curves shown in Fig. 2(b) exhibit a peak at an appropriate temperature and their shift with temperature is same as that of the P'_1 peak in Fig. 1(b). All of these characteristics of the P_0 and P''_1 peaks are consistent with experimental results in Ref. 9. However, the amplitude IF curves in the temperature range of the P''_1 peak are rather erratic, although anomalous amplitude dependence appeared.

To illustrate the anelasticity exhibited by the IF peaks, we choose the P'_1 peak as an example. In Fig. 3 shows the variation of the IF and modulus defect versus temperature at various measurement frequencies calculated at two strain amplitudes [(a) 3×10^{-6} , (b) 0.5×10^{-6}]. It can be seen that the temperature IF peak and modulus defect curve shift toward higher temperature with an increase of frequency, exhibiting the characteristic of relaxation type. Although the temperature dependence of the peak height at two strain amplitudes is different, as shown in Fig. 3, the apparent activation energies at two strain amplitudes calculated by the method of peak temperature shift with frequency are same and both consistent with the activation energy for dislocation core diffusion, i.e., 0.5 eV. Therefore the activation energy for dislocation core diffusion can be experimentally obtained by the nonlinear anelastic IF measurement.

ACKNOWLEDGMENTS

Thanks are given to Professor T. S. Kê for his helpful discussion in the process of building the physical model. This work has been subsidized by the National Natural Science Foundation of China (No. 59601008).

¹A. Granato and K. Lücke, J. Appl. Phys. **27**, 583 (1956); **27**, 789 (1956); **52**, 7136 (1981).

²T. S. Kê, Phys. Rev. **78**, 420 (1950).

³T. S. Kê, J. Alloys Compd. **211/212**, 90 (1994).

⁴T. S. Kê, Phys. Status Solidi A **155**, 83 (1996).

⁵W. Winkler-Gniewek, J. Schlipf, and S. Schindlmayer, in *Proceedings of ICIFUACS-5*, edited by D. Lenz and K. Lücke

(Springer-Verlag, Berlin, 1975), Vol. II, p. 246.

⁶T. S. Kê and Q. F. Fang, Phys. Status Solidi A **158**, 57 (1996).

⁷Q. F. Fang and T. S. Kê, Phys. Status Solidi A **158**, 405 (1996).

⁸Q. Tan and T. S. Kê, Phys. Status Solidi A **122**, K25 (1990).

⁹T. S. Kê, Q. Tan, and Q. F. Fang, Phys. Status Solidi A **103**, 421 (1987).